Original Research Article

DENDRITIC PRECIPITATES IN AS-CAST Nb-Ti-V MICROALLOYED STEEL

G. Basanta[a]*, A. L. Rivas[b], A. Costa e Silva [c], E. Dìaz[a]

[a]Instituto de Investigaciones Metalúrgica y de Materiales de la Siderúrgica del Orinoco (SIDOR), Puerto Ordaz, Estado Bolìvar, Venezuela. [b]Facultad de Ingeniería en Mecánica y Ciencias de la Producción- Escuela Superior Politécnica del Litoral., km 30.5 via Perimetral, Guayaquil-Ecuador, Dpto. de Ciencia de los Materiales, Universidad Simón Bolívar. Caracas, Venezuela. [c]EEIMVR-UFF, Volta Redonda, Rio de Janeiro, RJ, Brazil.

*Corresponding author, Email: gloriabasanta@gmail.com, phone: +58- 4249586266

Received: May 2017. Accepted: November 2017.
Published: December 2017.

ABSTRACT
The present research work deals with the analysis of dendritic precipitates present in a commercially produced Nb-Ti-V steel. The study was performed by scanning electron microscopy on precipitates extracted by chemical dissolution of a microalloyed steel matrix in the as-cast condition. Well-ramified dendritic precipitates of the (Ti,Nb,V)(C,N) type, rich in Ti or Nb of micrometric size, growing by faceted mechanisms were observed. The growth of primary and secondary arms look like laths when rich in Ti. This morphology is less accentuated in dendritic regions rich in Nb, which showed larger ramification. Dendrites with four-fold symmetry, with primary and secondary branches, were also found, but the well-ramified dendrites predominate. Computational thermodynamics was used to simulate the segregation during the solidification, and the results obtained both with the Scheil model and with a simple model including diffusion during solidification, are consistent with the observations.

Keywords: Microalloyed steels, dendritic precipitates, epitaxial growth, faceted growth.

INTRODUCTION

A good combination of strength and toughness in steels with improved weldability, can be achieved using microalloying, mainly by grain refinement mechanisms and precipitation hardening. This combination is more efficiently achieved if controlled rolling is used [1-4]. Thus, for instance, considerable increase in strength has been reported by Lu et. al [5] for precipitates with sizes lower than 5 nm. As in other steels, contributions to the strength are also provided by Mn, Si and other elements [3].

The most efficient use of microallying involves the proper combination of the microalloying elements Ti, Nb and V, when precipitation hardening is important [4]. Besides the concentration of the microalloying additions, the amount of C and N can influence the density, type and composition of precipitated particles, as well as the temperature range in which precipitation occurs. The effectiveness of using multi-element microadditions is strongly influenced by the nature and initial characteristics of the microalloy precipitates present in the continuous casting slab [6], as well as their dissolution and reprecipitation in the proper size distribution and with the correct composition. Thus, the composition, morphology, distribution and size of the precipitates in the as-cast plate may play a crucial role in controlling the microstructure of microalloyed steel during the hot rolling process, and on the steel performance. For this reason, many studies have been devoted to identify the types of precipitates present in the as-cast condition of the microalloyed steel-slab [6-9].

Carbonitrides of Ti, Nb and V in combination or along has a cubic structure, and they are are mutually soluble, to some extent, as a function of temperature and composition [1]. Furthermore, these elements segregate differently during solidification, and the steel may pass

through a peritectic transformation. When this occurs, austenite formation normally increases the segregation of various solutes [10]. Thus, precipitates of complex chemistry and morphology with sizes in the micrometric level can be found in as cast-plates. The most common coarse precipitates found in the as-cast structure of microalloyed steel-slab are of cuboidal shape, rich in Ti and N. In addition, precipitates with dendritic, laths and cruciform morphologies are also observed. Their characterization is complicated by the fact that some precipitation may occur during solidification while additional precipitation that happens on further cooling may (or may not) use the primary precipitates as nuclei. For instance, a study conducted by Baker et.al [11] evidenced large dendritic precipitates in V–Nb–Ti steels. Dendritic Ti, Nb carbonitrides in the as-cast slab microstructure, and TiN particles over 1 μm in size were also identified by Hong et. al [12] when studying a Ti-V-Nb steel. Cuboidal TiN, star-like (Ti, Nb)(C, N), and spherical NbC, were reported by Ruiz-Aparicio [13] in a low carbon microalloyed steel, with variation in Nb and Ti concentrations. Additionally, Li et. al [14], reported the observation of a eutectic carbonitride in a 0.22% C steel, after quenching from 1400°C. Cuboidal shaped TiN and round shaped mixed (Ti,Nb)(C,N) have been observed by Strangwood [15], while cruciform precipitates of complex (Ti,Nb)(C,N) were detected for instance by Ruiz-Aparicio [13] and by Kraven et al. [4]. Likewise, V-rich complex (Ti,Nb,V)(C,N) precipitates of different shapes were revealed by S. Shanmugam et al. [16].

The volume fraction of fine precipitates available in microalloyed steel to provide grain refinement and dispersion strengthening during thermomechanical processing, depends upon the amount of precipitates that can be taken into solution during reheating [17]. In conventional controlled hot rolling, continuous casting slabs frequently cool down to room temperature, follow by reheated up to 1250°C, to allow the homogenization of microstructure and the dissolution of precipitates formed during and after solidification. While a significant portion of the carbonitrides dissolve, the treatment cycle may be insufficient to dissolve some of the larger interdendritic carbonitrides completely. They may then remain partial or wholly undissolved after the typical reheating cycle [14], [18]. Knowing the content of microalloying elements that will be in solution at the end of the reheat cycle, is of great importance for the design of an efficient process and economical use of the microalloying elements.

Considering the reasons above depicted, the present work was conducted to evaluate the nature of large precipitates in a microalloyed steel slab, as well as the possible process involved in their formation. Even though considerable research has been done on the subject as discussed previously, the composition and morphology of the precipitates are, as expected, sensitive to chemical composition and casting parameters. Thus some near symmetric and well-developed dendritic precipitates morphologies reported in the present work have not been observed in the revised literature. In addition, the work shows results that indicate precipitate formation by epitaxial growth, similar to some observations reported by Ruiz-Aparicio [13]. In previous studies conducted by Basanta, et al. [19], complex carbonitrides precipitates were evaluated. New evidence of less conventional arrangements of dendritic precipitates will be the contribution of the present work.

MATERIALS AND METHODS

The study was performed upon a 200 mm thick Nb-Ti-V microalloyed steel-slab in the as-cast condition, produced by continuous casting. Table 1 displays the chemical composition of the microalloyed steel.

The characterization of precipitates was conducted on residues extracted from the matrix by chemical dissolution of the steel from samples cut from the centerline segregation area of the slab. The precipitates

collected in filters were analyzed by Scanning Electron Microscopy (SEM) and Energy Dispersive X-Ray Spectroscopy (EDS), through backscattered electron images mode, using ESEM FEI-Quanta FEG 250 with EDAX-APOLLO X and ESEM FEI-Quanta FEG 200 with Oxford-INCA. Computational thermodynamics calculations were performed with Thermo-calc 2016a and DICTRA [20], using TCFE8 [21] and MOBFE3 [22] databases.

Table1. Chemical composition of the microalloyed steel (Wt %)

Element	Wt %
C	0.12
Si	0.282
Mn	1.36
V	0.064
Nb	0.053
Ti	0.016
N	0.0064
S	0.003
Ti/N	2.5

RESULTS AND DISCUSSION

The SEM characterization of residues retained on filter paper after the dissolution of the matrix, revealed the presence of large and well-branched dendritic precipitates having secondary, tertiary and quaternary arms in the as-cast structure. Figure 1, for instance, shows a backscattered electron image of such precipitates, with a close-up of the right side zone at the upper part of this figure, which corresponds to a cuboidal precipitate. This precipitate grows by a faceted mechanism and degenerates in a dendrite with four primary arms, arising from the corners of the cuboid, which probably grow faster due to larger constitutional undercooling than on the facets, as suggested by Stefanescu [23]. The faceted cuboidal precipitate was identified as (Ti,Nb,V) (C,N) carbonitrides rich in Ti as revealed by the EDS analysis (a), taken in point (a) of Figure 1. A faceted secondary arm appears in one of the corner end of this cuboidal-particle, (point 2 in Figure 1), where there is probably more available space to growth. A similar developing process appears to be followed by other secondary arms, for example those numbered 3 to 6. A common characteristic to some of them, such as-those numbered 2, 4 and 6, is the change in the growth direction to a preferential crystallographic orientation, avoiding interference with surrounded secondary arms.

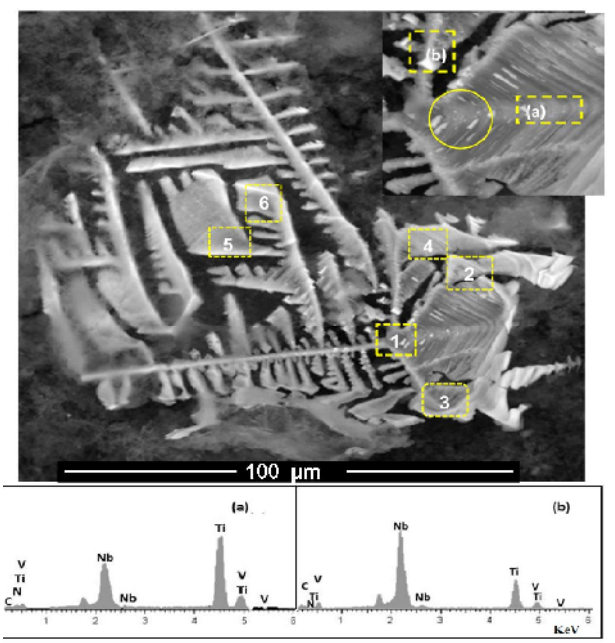

Fig.1. Dendritic Precipitate with EDS Analysis: a) EDS Analysis in pint a, b) EDS Analysis in pint b.

Closer examination of the cuboidal precipitate in Figure 1, provides more details about the faceted growth. It follows a stacking brick-like structure, probably due to a lateral growth mechanism from existing steps or ledges, along preferred growth direction, as pointed out by Cheng et al. [24] in a study on laser clad TiC reinforced FeAl intermetallic composite coating. Each layer is regularly spaced, and the spacing between them are distinguished by differences in contrast, suggesting fluctuations in chemical composition during the growing process. Inside the layers can be seen enlarged particles of few

microns, and finer rounded particles less than 1µm. Those particles are enclosed in a circle in Figure 1. Precipitate particles, as the brightest one labeled (b) in the magnified zone of Figure 1, are also observed on primary, secondary and tertiary arms. These brightest particles are rich in Nb, as showed by the EDS analysis (b), and may nucleate at lower temperatures in solid state given the reduction in the solubility of Nb, incrementing the stability of the Nb-carbonitride.

Analogs dendritic precipitates as the one showed in Figure 1, may be classified as precipitates type I, according to the description proposed by Baker [3]. They were located in the interdendritic zone [19], attributed to microsegregation, and originated by the rejection of microalloying elements by the growing solid. The rejected elements accumulate in front of the solid/liquid interface, leading to a decrease in the local freezing temperature by constitutional undercooling, generating the conditions for nucleation of microalloy-precipitates from the supersaturated liquid. The precipitates develop a dendritic morphology since any protuberance that is formed by the instability of solid/liquid interface, will survive in the undercooled liquid.

Some secondary and tertiary arms find more space for growth, experiencing a more marked coarsening. Likewise, the growth of secondary and tertiary arm is preferred at one side of some primary or secondary arm, respectively. The largest primary arm observed in Figure 1 is about 66 µm long. This dendrite shows near 19 secondary arms, including the tiny ones, given a secondary arm spacing of about 3.5 µm.

Figure 2 displays less-ramified dendrites. According to the mapping of microalloying elements of Figure 2a, the regions with fewer secondary arms are richer in Ti and contain Nb and V. The most ramified portions of dendrite are Nb-rich also containing Ti, and are depleted in V. The vanadium appears more associated to the Ti rich carbonitrides. According to Gobachev et.al [25], if the amount of Ti in steel is insufficient to bind nitrogen completely, then a noticeable amount of V can also be bound into corresponding carbonitride, which is the case of the steel under investigation. The microalloyed contains 0.0064 % of nitrogen and 0.016% of titanium. The stoichiometric amount of Ti required to binding this amount of nitrogen is 0.0219%. Therefore, the dissolution of V in Ti carbonotride can be justified. Additionally, the lattice parameter of titanium nitride and vanadium nitride are similar, 0.4244 nm [26] and 0.4139 nm [27], respectively. On the other hand, due to the significant differences in the lattice constants, V is unlikely to form a complex carbide with Nb, as pointed out by Inoue et al. [2]. Thus, the amount of V predicted in Nb carbonitrides is very limited.

A zone of Figure 2b enclosed in a circle, when magnified (Figure 2c), revealed the well-faceted growth of the dendrite, showing a lath-morphology again. It is important to highlight a lot of particles that precipitate inside the faceted precipitates, which also appear on its outer surface, and are observed with more detail on laths and cuboidal precipitates in Figure 3a and 3b. The formation of these Nb-rich precipitates on pre-existing Ti-rich precipitate, probably implied an epitaxial-growth mechanism, similar to NbC attached to a large cube-shaped (TiNb)(CN) reported by DeArdo in a Nb-Ti stabilized 409 Ferritic Stainless Steels [28] This preferential growth may be favor by a larger reduction in interfacial energy. In the present work, besides the cuboidal (Ti,Nb,V)(C,N) particles, these epitaxial precipitates also appear on laths and dendrites. They are of the (Nb,Ti,V)(CN) type, as exhibited by the semi-quantitative EDS analysis in Figure 3. The epitaxial growing precipitates attached to the outer surface of host particles are larger than those located in the interior. The bigger one is below 2 µm in

size. This suggests a faster-growing process on the free surface than in the interior of precipitate due to favored atom diffusion.

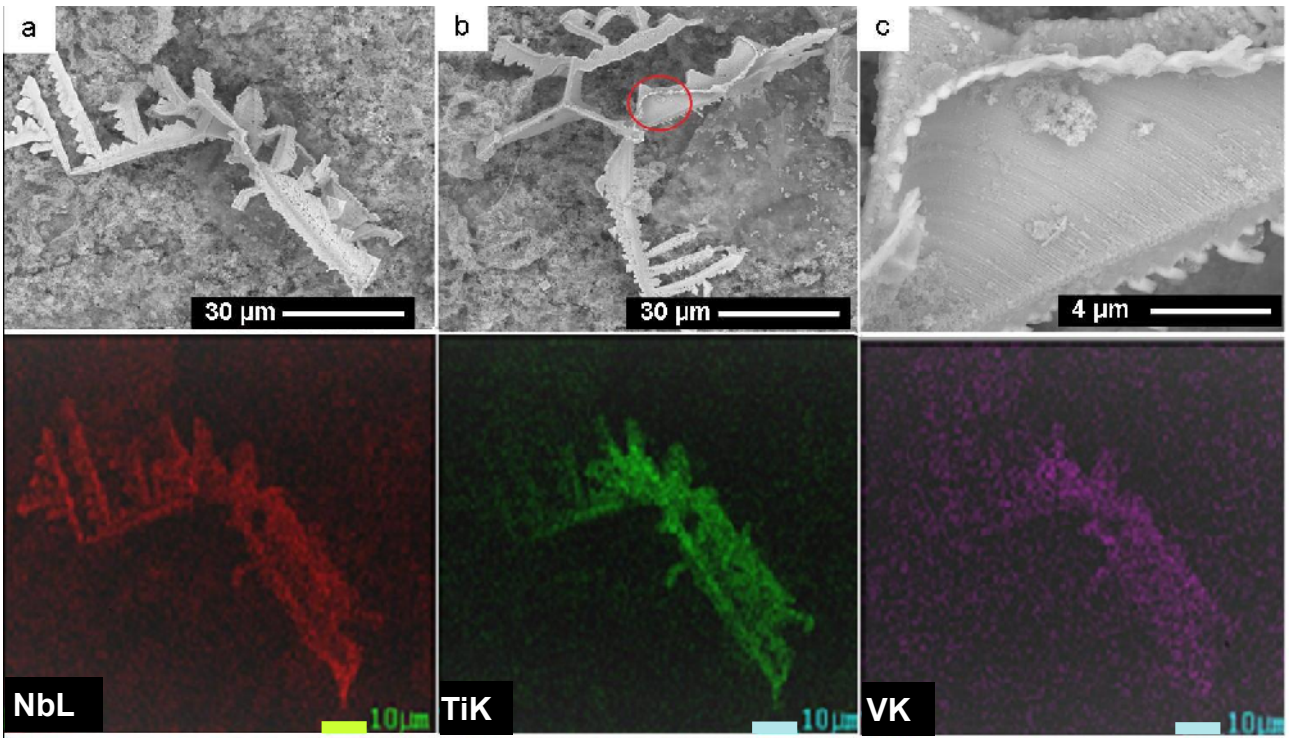

Fig. 2. Images of dendritic precipitates (a and b) with zapping of precipitate in image a. c) Detail of region encircled in b.

Figure 4a shows an image of dendritic carbide-particle, with primary branches forming an angle of 90° between them. The dendritic particle reflects a four-fold crystal lattice symmetry, and corresponds to a Nb-rich carbide, additionally containing Ti and V, as revealed by the EDS analysis, showing a ratio of composition close to Nb:Ti:V=0.84:0.12:0.04. It is important to notice that nitrogen was not detected in this particle. The dendritic precipitate ramified with a symmetric configuration of periodic secondary branched regularly spaced, growing perpendicular to the trunk of the primary arms. Small secondary arms, far from the tip, are less symmetric. The horizontal primary arm is near 5.6 µm long and the vertical one has a length of 4.2 µm, with 26 and 20 secondary arms, respectively, which gives a secondary arm spacing almost identical of about 0.2µm.

The development of this very symmetric dendritic morphology may be caused by an isotropic heat extraction for an undercooled melt, with an interface temperature gradient, G<0, [30]. The profile of heat extraction may be caused by local constitutional undercooling conditions around the distinct growing directions of the dendrite, free of interactions with another growing nucleus. The dendrite advance along fast growth directions, in this case <100> for a cubic crystal (cubic-F) [29].

Simulations with computational thermodynamics

The redistribution of solute during solidification has been modeled by several methods in the last decades with the aim of applying the models to the prediction of structure and chemical composition in continuously cast slabs (e.g.[31-34]). It is recognized that the

simplest model that can be applied to estimate the redistribution of solute is the one proposed by Scheil [35] in which complete mixing is assumed in the liquid and no diffusion in considered in the solid. Albeit this is an extreme situation, Schneider and co-workers [33] have achieved reasonable results when studying the precipitation of TiN in the centerline of continuous cast slabs. Furthermore, in recent years, a model in which carbon and nitrogen are considered to behave as if they could diffuse in the solid has been made available in by Chen and Sundman [36] and implemented in Thermo-calc. Within the methods of computational thermodynamics, the use of a diffusion simulation software such as DICTRA is the ideal solution [37]. However, the simulation of disperse solid phases precipitating from the liquid requires the use of the homogenization model [38] which, in the case of carbonitrides, can be extremely demanding on computational time. For this reason, two methods were used to evaluate the expected changes in the composition associated with segregation. In the first, segregation was simulated according to the Scheil model assuming C and N to diffuse according to [36].

The composition of the compounds identified as "TiN" and "NbC" are consistent with the miscibility gap calculated and measured by Inoue and co-workers in [2]. As the two compounds have the same crystal structure, epitaxy could be expected. Furthermore, as the growth happens in segregated liquid, the conditions for dendritic solidification are set, as discussed in the previous section. Different from the star-like or cruciform precipitates observed by Ruiz-Aparicio [13] however, it is evident that the solidification of the "NbC" compound can happen still in the liquid state, consistent with the microstructural observations described above. In both compounds, the calculations indicate small dissolution of vanadium, consistent with the lower stability of the carbonitrides of this element. It is most probable that the vanadium compound precipitates in the solid state on top of the particles formed in the liquid, in a mechanism similar to that described by Ruiz-Aparicio for star-like precipitates. However, this has not been detected by the SEM. This may be associated with the fact that they may be present at a finer size scale.

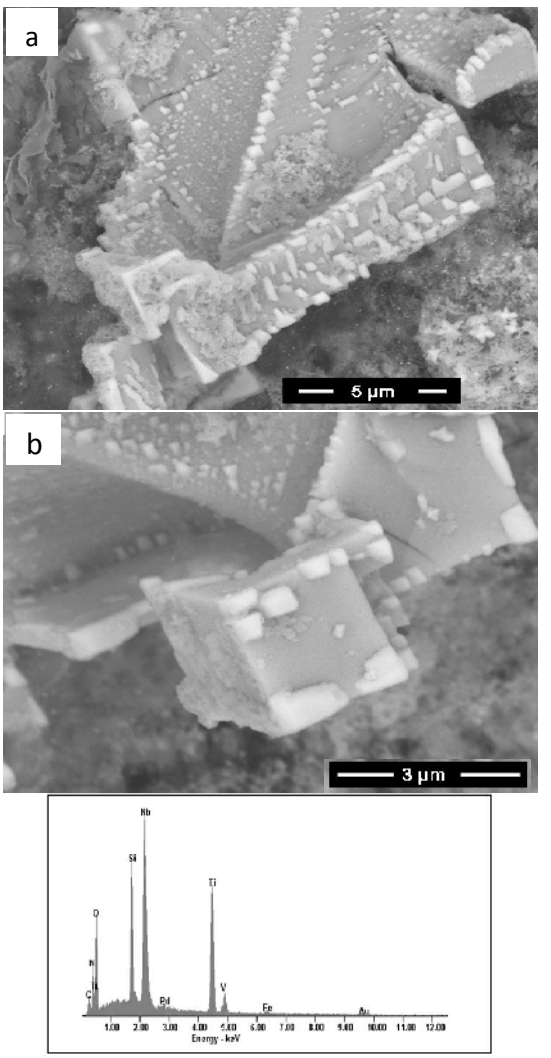

Fig. 3. Lath-Shaped Ti rich precipitates with EDS analysis of small Nb rich particles attached to them.

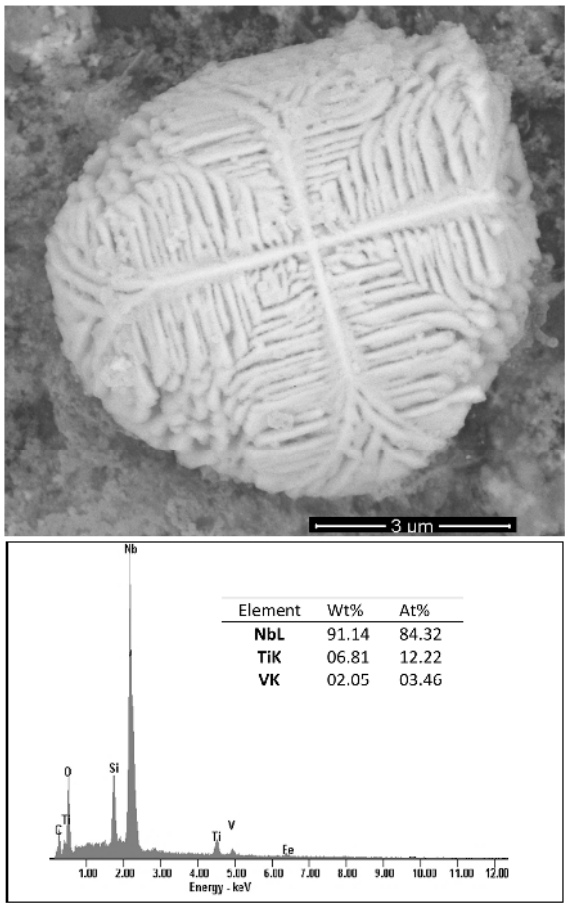

Fig. 4. Dendritic precipitate carbide with high symmetry growth, rich in Nb.

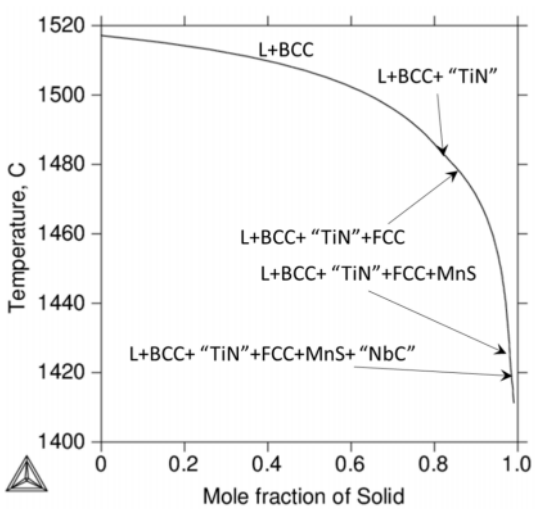

Fig. 5. Temperature versus fraction of solid in the Scheil simulation of the steel with the composition of Table 1. The temperatures at which each solid phase starts to precipitate are indicated with arrows.

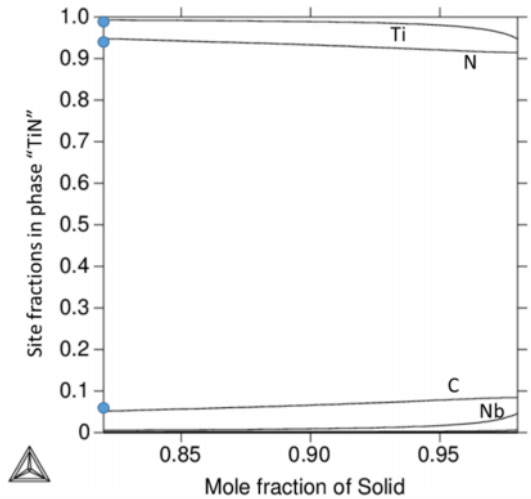

Fig. 6. Site fraction occupancy in $(Ti,Nb,V,Fe)_1(C,N,Va)_1$ in the compound identified as "TiN" in Figure 5 as a function of the mole fraction solidified. The dots indicate values calculated by DICTRA at the onset of precipitation, see text for discussion.

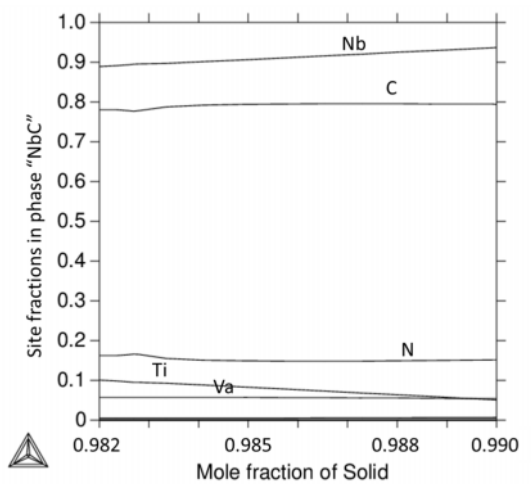

Fig. 7. Site fraction occupancy in $(Ti,Nb,V,Fe)_1(C,N,Va)_1$ in the compound identified as "NbC" in Figure 5 as a function of the mole fraction solidified.

In order to avoid the difficulties associated with the modeling of the precipitation of the carbonitrides in DICTRA, these phases were not included in the model. For a plate of 200 mm thickness, a secondary dendrite arm spacing of 575 μm was assumed. Using the correlations proposed by Suzuki and co-workers [39], this corresponds to a cooling rate of 0.03K/s. A cylindrical geometry was assumed with the secondary dendrite arm spacing as the diameter of the cylinder [37]. The simulation was conducted until complete

solidification. Then, the phases in equilibrium for each composition of the segregated liquid and temperature at the solid-liquid interface were calculated using Thermo-calc. The calculations indicated that "TiN" should start precipitating at 1488^{o}C compared with 1486 ^{o}C calculated by the Scheil model (Figure 5). Furthermore, the site fraction of the first compound precipitated from the liquid was compared with the composition calculated with the Scheil model and has shown good agreement (see Figure 6). From this point on, however, the calculated segregation using DICTRA would overestimate reality due to the absence of the precipitation of carbonitrides and thus is not presented here.

CONCLUSIONS

The as-cast Nb-Ti-V microalloyed slab contains large well-ramified precipitates of (Nb,Ti,V)(C,N) with faceted-dendritic morphology. The most faceted regions of the dendrites are richer in Ti. V is found more associated to Ti- rich precipitate than in Nb-rich particles. Small particles enriched in Nb growing by epitaxial mechanism, are found attached to laths precipitates. High symmetric dendrites with four-fold axis, can also form during casting. These are free of nitrogen-dendritic carbides. The simulation results with both the Scheil model and a simple model assuming diffusion during solidification, are consistent with the experimental results. In a paper to follow, dissolution of the dendritic precipitates will be addressed.

ACKNOWLEDGEMENT

The authors thank the Analytical Management of Electronic Microscopy Laboratory -INTEVEP for the use of the Scanning Electron Microscope and to SIDOR for the financial support.

REFERENCES

[1] T. Gladman. "*The physical metallurgy of microalloyed steels"* (1997). 1st ed. London: Institute of Materials pp.14, 103-134.

[2] K. Inoue, N. Ishikawa, I. Ohnuma, H. Ohtani and K. Ishida. (2001). "Equilibria between austenite and (Nb, Ti; V)(C, N) in microalloyed steels". ISIJ International. 41 175-182.

[3] T. N. Baker (2016). Microalloyed steels. "Ironmaking & Steelmaking". 43 264-307.

[4] A. J. Craven, K. He, L. A. J. Garvie and T. N. Bake (2000). "Complex heterogeneous precipitation in titanium–niobium microalloyed al-killed HSLA steels—I. (Ti,Nb)(C,N) particles". Acta Materialia. 48 3857–3868.

[5] J. Lu Wiskel, O. Omotoso, H. Henein and D.G. Ivey (2011). "Matrix Dissolution Techniques Applied to Extract and Quantify Precipitates from a Microalloyed Steel". Metallurgical and Materials Transactions A. 42 1767-1784.

[6] S. Roy, S. Patra, S. Neogy, A. Laik, S.K. Choudhary and D.Chakrabartt (2012). "Prediction of inhomogeneous Distribution of Microalloy Precipitates in Continuous-Cast High-Strength, Low-Alloy Steel Slab". Metallurgical and Materials Transactions A, 43 1845-1860.

[7] Z. Chen, M.H. Loretto and R.C Cochrane (1987). "Nature of large precipitates in titanium-containing HSLA steels". Materials Science and Technology. 3 836-844.

[8] X. Zhuo, X. Wang, W. Wang and H. G. Lee, (2007). "Nature of large (Ti, Nb)(C, N) particles precipitated during the solidification of Ti, Nb HSLA steel". Journal of University of Science and Technology Beijing: Mineral Metallurgy Materials. 14 112-117.

[9] S. Abraham, R. Klein, R. Bodnar and O. Dremailova (2006). "Formation of Coarse Particles in Steel as Related to Ferroalloy Dissolution Thermodynamics Part II: Crystallographic Study of Ferroalloys and Coarse Particles". Material Science and Technology (MS&T) Conference, TMS, Warrendale, PA, 109-122.

[10] M.G. Lage and Andre Costa e Silva, (2015). "Evaluating segregation in HSLA steels using computational thermodynamics". JMRT. 4 353–358.

[11] T.N. Baker, Y. Li, J.A. Wilson, A.J. Craven and D.N Crowther, (2004). "Evolution of precipitates, in particular cruciform and cuboid particles, during simulated direct charging of thin slab cast vanadium microalloyed steels". Materials Science and Technology. 20, 720-730.

[12] S.G Hong, H.J. Jun, K.B. Kang and C.G. Park, (2003). "Evolution of precipitates in the Nb-Ti-V microalloyed HSLA steels during reheating". Scripta Materialia. 48 1201-1206.

[13] A. Ruiz-Aparicio, (2004). "Evolution of Microstructure in Nb-Bearing Microalloyed Steels Produced by the Compact Strip Production Process". M. S. University of Pittsburgh. Thesis.

[14] P.H.Li, K.A Ibraheem and R. Prietsner (1998). "Eutectic Precipitation of (TiNbV)(CN) in Cast, Microalloyed Low-C Austenite and Effects of Reheating ". Materials Science, 284-286 517-524.

[15] C.L Davis and M. Strangwood, (2002). "Preliminary study of the inhomogeneous precipitate distributions in Nb-microalloyed plate steels". Journal of Materials Science. 37 1083-1090.

[16] S. Shanmugam, M. Tanniru, R.D.K. Misra, D. Panda and S. Jansto (2005). "Precipitation in v bearing microalloyed steel containing low concentrations of Ti and Nb". Materials Science and Technology, 21 883-892.

[17] J. Lu, O. Omotoso, B.J. Wiskel, D.G. Ivey and H. Henein, (2011). "Strengthening Mechanisms and Their Relative Contributions to The Yield Strength of Microalloyed Steels". Metallurgical and Materials Transactions A. 43 3035-3043.

[18] S. Zamberger, M. Pudar, K. Spiradek-Hahn, M. Reischl and E. Kozeschnik, (2012). "Numerical simulation of the evolution of primary and secondary Nb(CN), Ti(CN) and AlN in Nb-microalloyed steel during continuous casting". International Journal of Materials Research, 103(6) 680–7.

[19] G. Basanta, A.L Rivas and A. Ruiz, (2011). "A SEM Characterization of Complex Precipitates in an as-cast Nb-V- Ti-Microalloyed Steel". Rev. Latin Am. Metal. Mat. 31. 138-144.

[20] J. O. Andersson, T. Helander, L. Höglund P. Shi and B. Sundman, (2002). "Thermo-Calc & DICTRA, computational tools for materials science". Calphad. 26 273–312.

[21] TCAB, TCFE8, TCS Steel and Fe-alloys Database, Stockholm, 2015

[22] TCAB, MOBFE3 TCS Steels/Fe-Alloys Mobility Database, Stockholm, 2015.

[23] D. M Stefanescu, (2015). "*Science and Engineering of Casting Solidification"*. Kluwer Academic Plenum Publishers". New York, Boston, Dordrecht, London, Moscou. 3 145.

[24] Y. Cheng and H. Wuang, (2003). "Morphological evolution of TiC carbide in laser cladding modified Fe Al intermetallic composite coating". Transaction nonferrous Met. Soc. China. 13 835-838.

[25] I. I. Gorbachev, V.V. Popov, and A. Yu Pasynkov, 2014). "Thermodynamic Calculations of Carbonitride Formation in Low-Alloy Low-Carbon Steels Containing V, Nb, and Ti". The Physics of Metals and Metallography. 15 (69–76).

[26] K. Inoue, I. Ohnuma, H. Ohtani, K. Ishida and T. Nishizawa, (1998). "Solubility product of TiN in austenite. ISIJ international". 38(9), 991–997.

[27] T. Gendo, K. Morita, K. Inoue, I. Ohnuma, H. Ohtani and K. Ishida, (1998). "Solubility Product of VN in Austenite". (PRICM3) Proceeding of Third Pacific Rim International Conference on Advanced Materials and Processing, TMS. 3 229-234

[28] A.J. De Ardo, 2001. "Fundamental metallurgy of niobium in steel. Niobium. Science &

Technology". Int. Symp., Niobium, Orlando, Florida, USA, TMS. 427–478.

[29] Badeshia. Dendritic solidification. From http://www.msm.cam.ac.uk/phase-trans/dendrites.html ((accessed 07/11/ 2016)

[301] W. Kurz and D.J. Fisher, (1992). "Fundamentals of solidification". Trans Tech Publication. 3 67.

[31] T. Matsumiya, H. Kajioka, S. Mizoguchi Y. Ueshima and H. Esaka, (1984). "Mathematical analysis of segregations in continuously-cast slabs. Transactions of the Iron and Steel". Institute of Japan. 24 873–882.

[32] Y. M. Won and B.G Thomas, (2001). "Simple model of microsegregation during solidification of steels". Metallurgical and Materials Transactions A. 32. 1755–1767.

[33] A. Schneider, C. Stallybrass, J. Konrad, A. Kulgemeyer, H. Meuser and S. Meimeth, (2008). "Formation of primary TiN precipitates during solidification of microalloyed steels–Scheil versus DICTRA simulations". Int J Mat Res. 99 674-679.

[34] P. Schaffnit, C. Stallybrass, J. Konrad, F. Stein and Weinberg, (2015). "Scheil–Gulliver model dedicated to the solidification of steel". Calphad. 48 184–188.

[35] E. Scheil, (1942). "Uber die eutektische kristallisation". Zeitschrift Fur Metallkunde. 34. 70-80.

[36] Q. Chen and B. Sundman, (2002). "Computation of partial equilibrium solidification with complete interstitial and negligible substitutional back diffusion". Materials Transactions JIM. 43 551–559.

[37] A Costa e Silva, (2014). "Segregação Em Aços Alta-Resistência Baixa Liga (ARBL) Para Aplicações Em Serviço Com H2S: Avaliação por termodinâmica computacional". Revista Tecnologia em Metalurgia e Materiais, ABM. 11 3-13.

[38] H. Larsson and L. Höglund, (2009). "Multiphase diffusion simulations in 1D using the DICTRA homogenization model". Calphad. 33 495–501.

[39] A. Suzuki, A, T. Suzuki, Y. Nagaoka and Y. Iwata, (1968). "On secondary dendrite arm spacing in commercial carbon steels with different carbon content". Journal Japan Inst Metals. 32, 1301–1305.